P1.4

# RESULTS OF PHOTOCHEMICAL SIMULATIONS OF SUBGRID SCALE POINT SOURCE EMISSIONS WITH THE MODELS-3 CMAQ MODELING SYSTEM

James M. Godowitch*
Atmospheric Sciences Modeling Division
Air Resources Laboratory
National Oceanic and Atmospheric Administration
Research Triangle Park, North Carolina

## 1. INTRODUCTION

Plume-in-grid approaches have been incorporated into Eulerian air quality grid models to provide a more realistic treatment of the dynamic and chemical processes governing pollutants emitted from major point sources. Substantial emissions of nitrogen oxides ($NO_x$) and/or sulfur oxides ($SO_x$) are released from individual point sources into plumes with horizontal widths considerably smaller than the typical dimension of regional photochemical model grid cells (e.g. 20-40 km). Additionally, the pollutant mixture of fresh plumes from many point sources, particularly from fossil-fuel power plants, can be characterized to be in a high $NO_x$ / low VOC regime, while the ambient background surrounding a plume is often in the opposite chemical regime. The traditional Eulerian grid modeling approach has been to instantly mix point source emissions into an entire grid cell volume. This method, however, bypasses the diffusion-limited, chemical evolution occurring in subgrid scale plumes during transport downwind. The effect of this overdilution and the simultaneous availability of high $NO_x$ emissions and volatile organic compounds (VOCs) of anthropogenic and/or biogenic emissions in a grid cell are to promote the premature initiation of rapid photochemical production of secondary species, such as ozone ($O_3$). Since a plume-in-grid technique is designed to spatially resolve the subgrid scale concentration gradients in a plume and to simulate gradual plume growth in the horizontal and vertical in response to meteorological processes, photochemistry can be captured in a more realistic manner. Measurements of a variety of pollutants in plumes downwind of major point sources during recent field studies provide opportunities for plume-in-grid evaluation efforts to assess the capabilities of these subgrid scale plume treatments.

There have been a limited number of recent plume-in-grid efforts with a reactive plume algorithm being fully integrated into a 3-D photochemical grid model. A method with a plume composed of elliptical rings was embedded in the UAM-V model (Morris et al., 1992) and this same plume approach was incorporated in the SAQM model (Myers et al., 1996). Kumar and Russell (1996) developed and applied a plume model in the URM model with plume puffs treated for a limited period followed by the plume material being transferred into the grid. Karamchandani et al. (2000) described the SCICHEM / SCIPUFF plume model approach and they also presented evaluation results of their model against recent plume data.

A plume-in-grid (PinG) approach has been incorporated into the Community Multiscale Air Quality (CMAQ) modeling system (Byun et al., 1998). The CMAQ model system is composed of state-of-science meteorological, emissions, and air quality grid modeling components that reside in the Models-3 system framework (Novak et al., 1998). The latter also contains tools for model execution and for various analyses of model outputs. The PinG approach was specifically designed to address the need to more realistically resolve the spatial scale of plumes emanating from isolated, high emission point sources within an Eulerian coarse grid framework. The key science codes of the CMAQ plume-in-grid approach are a plume dynamics model (PDM) and a Lagrangian reactive plume model, which is designated as the PinG module since it is fully coupled with the CMAQ Chemical Transport Model (CCTM). An overview of these plume model components will be given.

The CCTM/PinG model was applied on a domain encompassing the greater Nashville, Tennessee region. Model simulations were performed for selected days in July 1995 during the Southern Oxidant Study (SOS) field study program, which was conducted in the Nashville area. In particular, five major point sources exhibiting a range of $NO_x$ emission rates were selected for the PinG treatment. Selected PinG model species concentrations and representative samples of the initial results of an ongoing evaluation of the PinG model with the SOS/Nashville 1995 data are presented to provide a preliminary demonstration of the capability of the CMAQ/PinG approach. In particular, modeled concentrations are compared to plume data for pollutant species collected during horizontal traverses by an instrumented helicopter and research aircraft across different plumes.

* Author address: J. Godowitch, US EPA, NERL, MD-80, RTP, NC 27711. On assignment to the EPA National Exposure Research Laboratory; e-mail: jug@hpcc.epa.gov

## 2. MODEL OVERVIEW

The PinG approach is based on the Lagrangian reference frame with a continuous plume represented by a series of moving plume sections released at hourly intervals from the location of a point source. The PinG module simulates one or multiple point source plumes and is designed to treat the physical and chemical processes during the entire diurnal cycle. The PDM processor generates plume dimensions, plume section position on the grid, and other relevant parameters needed by the CCTM/PinG. The Lagrangian PinG module is fully coupled with the CCTM and is executed simultaneously with the grid model (Godowitch et al., 1999). Horizontal resolution across a plume section is achieved with a contiguous array of attached plume cells. Currently, each plume section is composed of 10 plume cells in addition to a left and a right boundary cell. The plume boundary conditions, representing the ambient background, are provided throughout the simulation by the appropriate CCTM grid cell concentrations. In the current PinG version, the plume cells represent a single vertical layer. Plume cells in a plume section have the same plume bottom and a common top height.

Relevant processes have been incorporated into the plume equation for the mass balance of individual pollutant species in each plume cell. The key plume processes include dilution and entrainment due to vertical expansion, dilution and entrainment / detrainment from horizontal expansion, crosswind plume diffusion between plume cells, gas-phase chemistry, surface dry deposition, and surface emissions. The detailed mathematical formulation of these processes is documented in Gillani and Godowitch (1999).

Since plume chemical evolution is strongly influenced by plume expansion, plume growth must be realistically simulated with time after release. The PDM processor determines plume rise and provides the plume dimensions and growth rate parameters for use by PinG in the physical processes mentioned above. Parameterizations are employed in PDM to determine the turbulence and wind shear contributions to plume growth based on 2-D and 3-D meteorological fields generated by the Penn State/NCAR mesoscale model (MM5). For consistency with the grid model, PinG applies the same gas-phase chemical mechanisms and chemical solvers used by the CCTM. Currently, the RADM2 or CB-4 chemical reaction schemes can be selected for photochemistry. The chemical solvers include a quasi-steady state (QSSA) method and the sparse-matrix vectorized Gear (SMVGEAR) technique (Gipson and Young, 1999). PinG also applies the same pollutant deposition velocities used by the CCTM for dry deposition and surface emission fluxes are injected into the surface-based plume sections. Plume transport is determined from mean wind components, which are computed by averaging winds from model layers spanned by each plume section.

## 3. MODEL SIMULATIONS AND RESULTS

The Eulerian modeling domain used in the CCTM/PinG simulations consisted of 21 x 21 horizontal grid cells with a 36 km grid cell size and 21 vertical layers. This model domain was centered on the greater Nashville, Tennessee area and it covered most of the southeastern US. It also is a subdomain of a much larger 36 km gridded modeling domain encompassing the entire eastern half of the US. By using a subdomain targeted on the experimental study region of interest, the computational time and file sizes were greatly reduced. Additionally, initial and boundary conditions for this subdomain were provided from CCTM modeled concentrations already generated from simulations on the large domain. Likewise, meteorological and emissions data sets for this application were extracted from data files for the larger domain using existing CMAQ processor programs. The CCTM/PinG simulations were for 24-hour periods starting at 00 GMT. The model results to be shown were obtained from simulations using the CB-4 chemical mechanism and QSSA solver, which required less computational time than the RADM2 mechanism.

A set of five major $NO_x$ point sources was selected for the plume-in-grid treatment. The point source emissions treated in PinG were from the Shawnee (SH), Paradise (PA), Cumberland (CU), Johnsonville (JV), and Gallatin (GA) fossil-fuel power plants. Continuous Emissions Monitoring (CEM) data from the 1995 NET (National Emission Trends) inventory provided the hourly emissions for each point source. All other point sources in the domain were modeled with the traditional Eulerian grid treatment and were included the 3-D emissions input data file. Based on the total daily $NO_x$ emissions for a typical day (e.g., July 7, 1995), the lowest to highest $NO_x$ emission sources were GA, SH, JV, CU, and PA. Using GA as a reference source (32 tons of $NO_x$/day), the daily $NO_x$ emissions from SH, JV, CU, PA were a factor of 3.0, 3.7, 15.0, and 15.2 times higher, respectively. The PinG results from model simulations for July 7 and July 16, 1995 are emphasized in this paper because the CU plume, in particular, was sampled extensively at various downwind distances during afternoon hours by the instrumented airborne platforms.

### 3.1 Selected Results From PinG Simulations

The evolution of ozone ($O_3$) and nitrogen oxide (NO) concentrations in a plume section released at 1400 GMT (i.e., 0900 local daylight time) from CU and JV are displayed in Figures 1 and 2, respectively. The set of both figures illustrates the typical daytime chemical evolution occurring in rather large, isolated power plant plumes, which

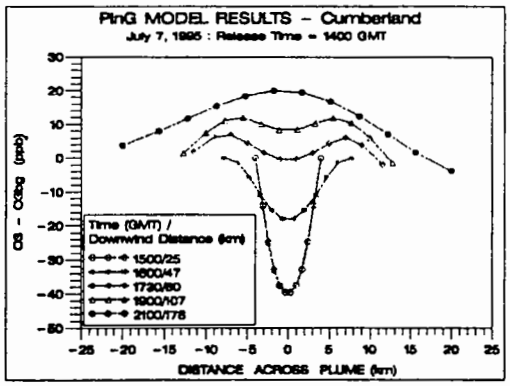


Figure 1a. Ozone concentrations relative to background values in the CU plume section released at 1400 GMT for various times and downwind distances on July 7, 1995.

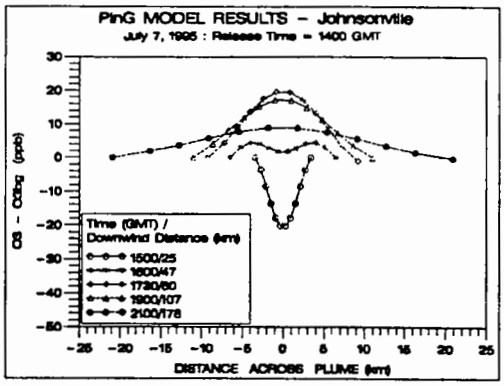


Figure 2a. Ozone concentrations relative to background levels in the JV plume section released at 1400 GMT on July 7, 1995.

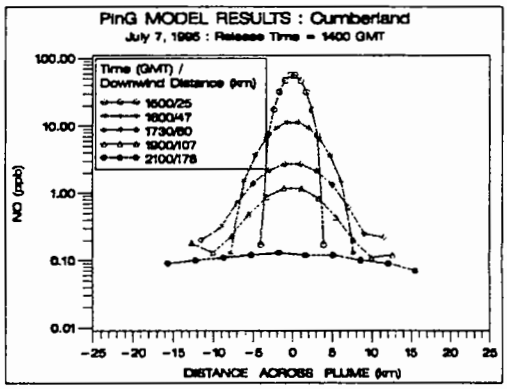


Figure 1b. Same as in Fig.1a, except for NO concentrations in the CU plume section.

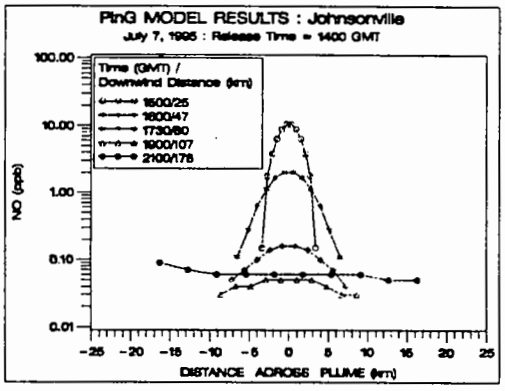


Figure 2b. Same as Fig. 2a, except for NO concentrations in the JV plume section.

consists of three distinct stages. In stage 1, the relatively fresh plume is dominated by primary emissions, and a deficit of $O_3$ relative to surrounding ambient background concentrations exists in the plumes due to substantial titration from NO. As a plume expands and experiences mixing with background concentrations, in this case provided by the CCTM gridded concentrations, a transition to stage 2 occurs with rapid $O_3$ production near the plume edges. During this stage, a plume displays the characteristic 'wings' near the plume edges as elevated $O_3$ values exceed background values. Ozone concentrations in the plume core also exhibit a strong recovery but remain depressed relative to those found further from the plume centerline. In stage 3, the plume sections from both point sources have experienced considerable dilution due to horizontal expansion and are chemically mature. A noticeable $O_3$ bulge is found across the entire plume. The plume sections from both sources exhibit $NO_x$-limited conditions in stage 3 as NO concentrations have been reduced to near background values.

It is also apparent from these figures that the $O_3$ recovery and chemical evolution in the JV plume section is more rapid than for the CU plume section. The notable difference between these plume sections was that the NO emission rate at JV was considerably lower, by about a factor of 4, than from CU at this release time and the NO concentration differences between these plume sections reflect this emission rate difference. Results of PinG model results in Godowitch and Young (2000) revealed the $NO_x$ oxidation rate was inversely related to the $NO_x$ emission rate. Thus, slower $NO_x$ oxidation rates occurred in the modeled plumes from the highest $NO_x$ point source emissions. This feature has also been supported by plume observational results from these same point sources in Ryerson et al. (1998).

The temporal behavior of $O_3$ in the plume core for the 1400 GMT release is depicted in Figure 3 for three of the point sources to demonstrate the impact from different $NO_x$ emission rates. It is

evident that the time required for $O_3$ in the plume core to recover to the background value and the time of occurrence of the peak $O_3$ differ greatly depending on the $NO_x$ emission rate. Ozone in the GA plume with the lowest $NO_x$ emission recovered quickest and reached maturity fastest, although it also exhibited the lowest peak $O_3$ relative to background compared to either JV or CU. In this case, the CU plume section required almost 4 hours for $O_3$ in the plume core to reach background levels and about 6 hours of travel time to reach its peak value of about 20 ppb above background. Interestingly, the JV plume section also achieved a peak $O_3$ value of about 20 ppb above background, however, it occurred much sooner after release than the CU peak value. This indicates the CU peak $O_3$ was found much further downwind. These model results are also comparable to observational results in Ryerson et al. (1998) who reported plume ozone exceeded background by as much as 23 ppb. They also noted the peak $O_3$ was found closer to the source for the JV plume based on aircraft traverses downwind of JV and CU during the afternoon of July 7.

A similar plot for $NO_z$, representing the sum of all nitrogen species generated in the photochemical process, relative to background levels is depicted in Figure 4. Photochemical production leads to higher $NO_z$ levels as $NO_x$ source strength increased. The peak $NO_z$ values also occurred concurrently with peak $O_3$ values. Additionally, it is evident that photochemical production of nitrogen species occurs more rapidly after release since $NO_z$ exceeds background levels in each point source plume section within an hour after release. Nitric acid ($HNO_3$) made up the largest fraction of $NO_z$ in these plumes.

### 3.2 Comparisons of Model and Observed Species Concentrations in Plumes

Plume concentrations generated from CCTM/PinG simulations are compared directly to observed species concentrations obtained during aircraft and helicopter flights from the SOS field study in the Nashville region. The weather conditions during July 7, 1995 were quite favorable for experimental sampling of isolated major point source plumes in the greater Nashville area. With a steady northwesterly wind flow with speeds of 5-7 m/s in the afternoon convective boundary layer, the plumes from the major point sources remained separated from each other and from the Nashville urban area (Godowitch and Young, 2000), which would have complicated interpretation of results.

The PinG modeled concentrations from plume sections closest in time and space to the plume measurements made during a horizontal flight path on July 7th (Nunnermacker et al., 2000) by the Department of Energy (DOE) G1 research aircraft are displayed in Figure 5. The modeled concentrations of superimposed $O_3$, $SO_2$, and $NO_y$ (sum of all nitrogen species) are on the plumes

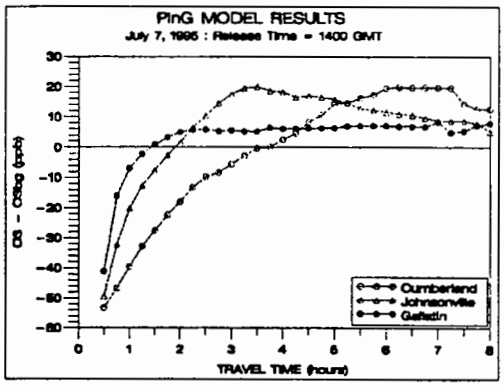


Figure 3. Variation of ozone in the plume core relative to background with time after release for the plume section emitted at 1400 GMT from the different point sources.

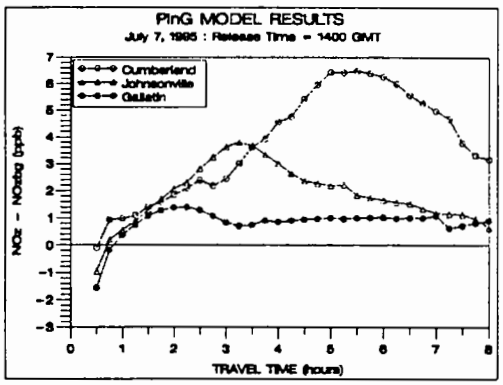


Figure 4. Same as in Fig. 3, except for plume $NO_z$ after removing the background value.

intercepted at about 46 km and 36 km downwind of JV and CU, respectively, during the aircraft flight. The pollutant signature of each plume reflects the impact of primary emissions from each point source. Relatively high $SO_2$ emissions compared to lower $NO_x$ emissions exist at JV, whereas CU emits relatively high $NO_x$ emissions compared to low $SO_2$ emissions. The PinG model concentrations of $SO_2$ and $NO_y$ are strongly supported by the data obtained through each plume, which suggests the emissions were accurately specified and the plume dispersion and chemistry processes, in particular, were treated realistically out to these downwind distances. It is also encouraging that the PinG model simulates the plume $O_3$ rather closely at these distances for both sources with Figure 5 showing a mature JV ozone plume while the CU plume still displays an ozone deficit.

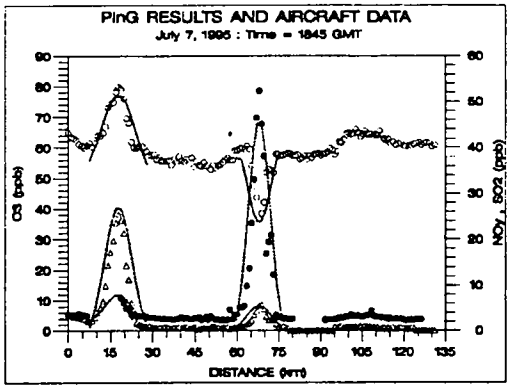


Figure 5. Comparison of PinG concentrations for ozone (solid lines) , $NO_y$ (short dashed lines), and $SO_2$ (long dash) versus measured $O_3$ (o), $SO_2$ ($\Delta$) and $NO_y$ (•) from the DOE aircraft flight across the JV (extreme left plume) and CU plume on the afternoon of July 7, 1995. Interceptions of the JV and CU plumes were made at downwind distances of 46 km and 36 km, respectively.

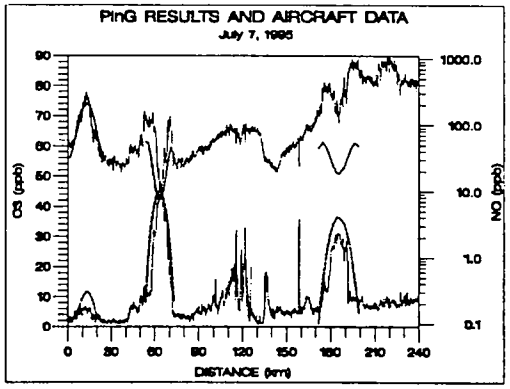


Figure 6. Comparison of PinG ozone (thick solid lines) and NO (dashed lines) concentrations for the JV, CU and PA plumes (from left to right) vs. the NOAA WP-3 aircraft data sampled at 1-s intervals at about 80 km downwind of JV and CU, and about 100 km downwind of PA for the horizontal traverse starting at 2006 GMT on July 7, 1995.

Another model/aircraft data comparison is depicted in Figure 6, which contains the data collected during traverse 3 of the NOAA WP-3 aircraft flight on July 7th (Ryerson et al., 1998). The flight path was along a SW to NE line across the region and intercepted the JV, CU, and PA plumes from left to right in Figure 6. PinG model concentrations of $O_3$ and NO are very comparable for the JV and CU plumes at 80 km downwind. However, for the modeled PA plume, a notable underestimate in $O_3$ exists, although the plume $O_3$ structure is similar to the observed plume. This shift in the magnitude of $O_3$ for the modeled PA plume is largely attributable to underpredicted boundary concentrations provided by the grid model. It became apparent from an examination of the observed $SO_2$ concentrations (not shown here) and this $O_3$ data series that another mature plume from a major point source further upwind of PA exists on the right of the PA plume in Figure 6. This example demonstrates the impact on the PinG model from grid model boundary conditions.

Measurements made during several horizontal traverses of the CU plume at different downwind distances from the TVA helicopter flights on the afternoon of July 7th are compared to PinG concentrations. Figure 7a displays in-plume $O_3$ concentrations after subtracting model background values. Likewise, Figure 8a contains the observed in-plume $O_3$ structure after subtracting observed background values. In addition, the plume width from the centerline to each edge was employed to normalize the distance across each side of the observed and model plumes at these different downwind positions. The modeled evolution and magnitudes for ozone and $NO_y$ shown in Figure 7a and 7b are quite similar with the observed patterns depicted in Figures 8a and 8b.

Statistical results computed from paired model and observed plume concentrations from helicopter sampling on July 7 and 16, 1995 are presented in Table 1 and 2, respectively. Owing to differences between model and observed background values of $O_3$ in these cases, $O_3$ background values were subtracted in order to focus on the relative $O_3$ concentrations in the modeled and observed plumes for this species. This procedure was not performed for other pollutants. Concentrations of NO, in particular, are noticeably lower for the slower wind case on July 16, which is indicative of a somewhat 'older' plume at the same downwind distance. More quantitative results at other downwind distances for various species are expected to provide a better overall picture of model performance.

## 4. SUMMARY AND ONGOING WORK

Model simulations of the CCTM/PinG have been performed to provide modeled plume species concentrations from selected major point sources for quantitative comparisons with plume measurements from the SOS summer 1995 Nashville field study. These initial results and comparisons of modeled and observed plume concentrations are encouraging with the PinG model exhibiting the capability of realistically simulating the observed photochemical behavior for $O_3$ and other species for these case studies. Similar analyses will be performed for other case study days. Additional PinG simulations are also anticipated with a CCTM fine grid (e.g. 12 km) domain and with the RADM2 chemistry mechanism.

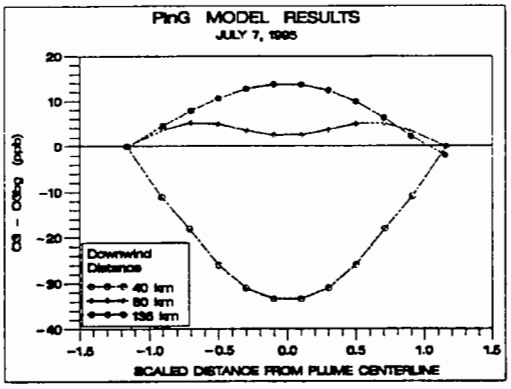


Figure 7a. PinG model ozone concentrations relative to background in the CU plume at downwind distances corresponding to the observed plumes on the afternoon of July 7, 1995 shown in Fig. 8a. Position within each plume has been normalized by the distance from plume centerline to each edge for each downwind distance.

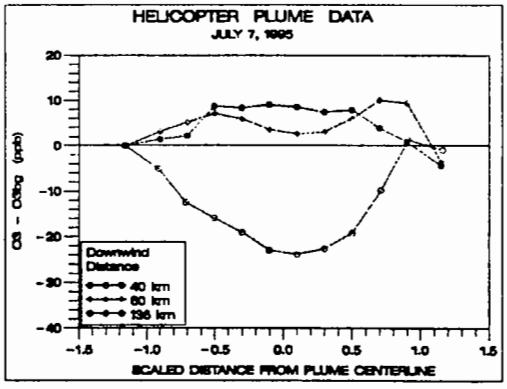


Figure 8a. Observed ozone relative to background in the CU plume at three downwind distances from horizontal plume interceptions by the TVA helicopter during the afternoon of July 7, 1995.

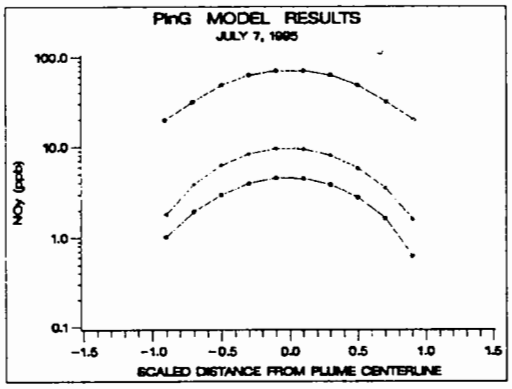


Figure 7b. Same as in Fig. 7a, except for total nitrogen species ($NO_y$) concentrations.

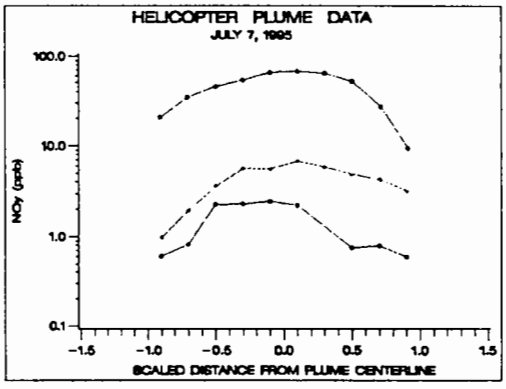


Figure 8b. Same as in Fig. 8a, except for observed $NO_y$ concentrations.


## ACKNOWLEDGEMENT

Thanks are due to the NOAA Aeronomy Laboratory for submitting the WP-3 aircraft data and to the Dept. of Energy for providing the G1 aircraft data to the EPA SOS data base. Appreciation is due to the TVA Atmospheric Sciences and Environmental Assessments Dept. for providing the helicopter plume model evaluation data set.


## DISCLAIMER

This paper has been reviewed in accordance with the U.S. Environmental Protection Agency's peer review and administrative review policies and approved for publication. Mention of trade names or commercial products does not constitute endorsement or recommendation for use.

## REFERENCES


Byun, D., et al., 1998: Description of the Models-3 Community Multiscale Air Quality (CMAQ) Modeling System, 10th Joint Conf. on Applications of Air Poll. Meteorol. with A&WMA., 11-16 Jan. 1998, Phoenix, AZ, p 264-268.

Gillani, N.V. and J.M. Godowitch, 1999: Plume-in-grid treatment of major point source emissions. Chap. 9, EPA/600/R-99/030, Research Triangle Park,NC, URL://http://www.epa.gov/asmdnerl/models3/doc/science

Gipson, G. and J.O. Young, 1999: Gas-phase chemistry, Chap. 8, EPA/600/R-99/030, Research TrianglePark,NC, URL:http://www.epa.gov/asmdnerl/models3/doc/science/

Godowitch, J.M., et al., 1999: Photochemical plume-in-grid simulations of major point sources in the CMAQ modeling system, Symp. on Interdisciplinary Issues in Atmos. Chem., 10-15 Jan. 1999, Dallas, TX, p 121-124.

Godowitch, J.M. and J.O. Young, 2000: Photochemical simulations of point source emissions with the Models3 CMAQ plume-in-grid approach., A&WMA 91st Annual Conf., 18-22 June 2000, Salt Lake City, UT., 14 pp.

Karamchandani, et al., 2000: Development and evaluation of a state-of-science reactive plume model, Environ. Sci. Technol., 34, 870-880.

Kumar, N. and A.G. Russell, 1996: Development of a computationally efficient reactive subgrid-scale plume model, J. Geophys. Res.,101, 16737-16744.

Morris, R.E., et al., 1992: Overview of the variable-grid UAM-V. A&WMA 85th Annual Conf., June 1992, Kansas City, MO.

Myers, T., et al., 1996: The implementation of a plume-in-grid module in SAQM. Report SYSAPP-96-/06, Systems Applications Intl., San Rafael, CA.

Novak, J.N., et al., 1998: Models-3: A unifying framework for environmental modeling and assessment. 10th Joint Conf. on Appl. Of Air Poll. Meteorol., 11-16 Jan. 1998, Phoenix, AZ.

Nunnermacker, L. J., et al., 2000. NOy lifetimes and O3 production efficiencies in urban and power plant plumes: Analysis of field data, J. Geophys. Res., 105, 9165-9176.

Ryerson, T. B., et al., 1998: Emissions lifetimes and ozone formation in power plant plumes. J. Geophys. Res., 103, 22569-22583

**Table 1. Statistics of PinG model results and observed helicopter concentrations in the Cumberland plume at 40 km downwind on July 7, 1995 (1517 – 1630 GMT)**

| | Model | Observed | Peak | | |
|---|---|---|---|---|---|
| Species | Ave SD | Ave SD | Model Obs | Bias | R |
| O3 - O3bg | -24.2 ± 56.1 | -18.3 ± 41.7 | -5.7 1.3 | -5.9 | 0.86 |
| NO | 22.2 ± 89.1 | 17.6 ± 57.8 | 59.7 39.6 | 4.7 | 0.96 |
| NOy | 49.1 ±143.8 | 42.5 ±112.0 | 103.2 79.6 | 6.6 | 0.95 |
| SO2 | 5.2 ± 14.7 | 3.7 ± 12.2 | 10.7 7.4 | 1.5 | 0.72 |

**Table 2. Statistics of PinG model results and observed helicopter concentrations in the Cumberland plume at 36 km downwind on July 16, 1995 (1748 – 1951 GMT)**

| | Model | Observed | Peak | | |
|---|---|---|---|---|---|
| Species | Ave SD | Ave SD | Model Obs | Bias | R |
| O3 - O3bg | -4.8 ± 81.4 | 0.8 ± 79.8 | 11.5 22.9 | -5.6 | 0.76 |
| NO | 5.9 ± 33.2 | 7.4 ± 40.4 | 17.1 21.3 | -1.5 | 0.74 |
| NOy | 30.2 ±115.3 | 25.5 ±111.0 | 65.5 55.9 | 4.7 | 0.79 |
| SO2 | 4.8 ± 18.2 | 3.4 ± 13.2 | 10.4 7.0 | 1.4 | 0.70 |

Note: Bias = Model – Observed , SD = standard deviation , R = correlation coefficient
Concentration units = ppb

NERL-RTP-AMD-00-208

TECHNICAL REPORT DATA

| 1. REPORT NO. | 2. | 3.RECIPIENT'S ACCESSION NO. |
|---|---|---|
| EPA/600/A-00/114 | | |

| 4. TITLE AND SUBTITLE | 5.REPORT DATE |
|---|---|
| RESULTS OF PHOTOCHEMICAL SIMULATIONS OF SUBGRID SCALE POINT SOURCE EMISSIONS WITH THE MODELS-3 CMAQ MODELING SYSTEM | 6.PERFORMING ORGANIZATION CODE |

| 7. AUTHOR(S) | 8.PERFORMING ORGANIZATION REPORT NO. |
|---|---|
| James M. Godowitch | |

| 9. PERFORMING ORGANIZATION NAME AND ADDRESS | 10.PROGRAM ELEMENT NO. |
|---|---|
| Same as Block 12 | 11. CONTRACT/GRANT NO. |

| 12. SPONSORING AGENCY NAME AND ADDRESS | 13.TYPE OF REPORT AND PERIOD COVERED |
|---|---|
| U.S. Environmental Protection Agency<br>Office of Research and Development<br>National Exposure Research Laboratory<br>Research Triangle Park, NC 27711 | Proceedings, FY-01 |
| | 14. SPONSORING AGENCY CODE<br>EPA/600/9 |

15. SUPPLEMENTARY NOTES

16. ABSTRACT

The Community Multiscale Air Quality (CMAQ) / Plume-in-Grid (PinG) model was applied on a domain encompassing the greater Nashville, Tennessee region. Model simulations were performed for selected days in July 1995 during the Southern Oxidant Study (SOS) field study program which was conducted in the Nashville area. In particular, five major point sources exhibiting a range of NOx emission rates were selected for the PinG treatment. Selected PinG model concentrations and representative examples of the initial results of an ongoing evaluation of the PinG model with the SOS/Nashville data are presented to provide a preliminary demonstration of the capability of the CMAQ/PinG approach. In particular, modeled concentrations of ozone, SO2, and nitrogen oxides are compared to plume data collected during horizontal traverses by an instrumented helicopter and research aircraft across different plumes. Statistical results are also provided at 40 km downwind of the largest point source. The comparisons and quantitative results are encouraging as PinG exhibited the capability to realistically simulate the observed photochemical evolution for ozone and other species at various downwind distances for these cases.

17. KEY WORDS AND DOCUMENT ANALYSIS

| a. DESCRIPTORS | b.IDENTIFIERS/ OPEN ENDED TERMS | c.COSATI |
|---|---|---|
| | | |

| 18. DISTRIBUTION STATEMENT | 19. SECURITY CLASS *(This Report)* | 21.NO. OF PAGES |
|---|---|---|
| RELEASE TO PUBLIC | UNCLASSIFIED | 7 |
| | 20. SECURITY CLASS *(This Page)* | 22. PRICE |
| | UNCLASSIFIED | |